Ionizational Nonequilibrium in Thermal Air Plasmas

Christophe O. Laux, Richard J. Gessman, and Charles H. Kruger

High Temperature Gasdynamics Laboratory
Stanford University – Stanford, CA 94305-3032 – USA

Abstract

Experimental and numerical investigations are presented of the mechanism and degree of ionizational nonequilibrium in recombining thermal plasmas of air and nitrogen. It is shown that electron recombination occurs primarily via inherently fast and equilibrated two-body dissociative recombination reactions, and therefore that ionizational nonequilibrium in molecular plasmas is generally not due to finite three-body electron recombination rates, but rather to slow neutral recombination. Numerical simulations performed with various reaction mechanisms are compared with measurements conducted in air and nitrogen plasmas generated by a 50 kW RF plasma torch. The results support the proposed recombination model and provide a preliminary assessment of the rates of importance in the chemistry of recombining plasmas.

Introduction

Many plasma processing applications involve expanding, cooling molecular thermal plasmas. If ionizational nonequilibrium in the form of electron number densities elevated with respect to equilibrium occurs in such plasmas, the reactivity and transport properties may be greatly affected. In addition, collisional coupling between the populations of bound and free electrons may perturb the radiative phenomena and thereby complicate the interpretation of optical diagnostics. It is therefore important to understand the mechanism of electron recombination in molecular plasmas.

Departures from equilibrium in the population of free-electrons in thermal plasmas are normally attributed to finite rates for three-body electron recombination. Indeed, in atomic or fully dissociated molecular plasmas (e.g., atmospheric pressure air or nitrogen above ~10,000 K) electrons recombine via reactions of the type $X^+ + e + M \Leftrightarrow X + M$ (where M is a third-body electron or heavy particle) which tend to be relatively slow as they involve ternary collisions. If molecular ions are present in the plasma (air, nitrogen below ~10,000 K), electrons can recombine instead via the dissociative recombination reactions $XY^+ + e \Leftrightarrow X + Y$. The latter reactions are typically much faster (only two collision partners are involved) and equilibrate more rapidly than three-body electron recombination reactions. Moreover, charge exchange reactions are

usually fast as well. As a result, the preferential channel for electron recombination in molecular plasmas is via dissociative recombination. The degree of ionizational nonequilibrium is then determined by the rates of (three-body) atomic recombination reactions $X + Y + M \Leftrightarrow XY + M$. In general, these reactions are relatively slow and thus tend to be the limiting step for electron recombination. Hence the result, suggested earlier in Ref. [1], that ionizational nonequilibrium in molecular plasmas is caused by finite-rate neutral chemistry. Reliable rates for atom recombination reactions are therefore required to accurately predict the extent of ionizational nonequilibrium in molecular plasmas. Unfortunately, at present many of these rates are not known with good accuracy, in particular in the temperature range below 7000 K which is of interest to various plasma processing applications.

The purpose of this paper is to provide an experimental assessment of the recombination model and of the various reaction mechanisms proposed in the literature. Temperature, electron and heavy particle concentrations were measured in recombining air and nitrogen/argon plasmas produced by a 50 kW RF plasma torch operating at atmospheric pressure. The results are compared with kinetic simulations based on three widely used reaction mechanisms [2-4]. The influence of ionizational nonequilibrium on the interpretation of optical diagnostics is briefly discussed.

Experimental Facility

A 50 kW TAFA model 66 RF induction plasma torch, powered by a LEPEL model T-50-3 power supply operating at a frequency of 4 MHz, is used to generate a flowing plasma at atmospheric pressure. The plasma produced in the torch exits through a 1 cm diameter copper nozzle at a velocity approaching 1 km/s. It then flows through a water-cooled, 1 cm diameter brass test-section mounted on the exit nozzle of the torch as shown in Fig. 1. The test-section consists of two brass tubes separated by a 3 mm thick annular water cooling passage. Within the test-section, the plasma is forced to recombine in a well-controlled environment over a predetermined residence time. Several test-sections with lengths between 10 and 25 cm in 5 cm increments were used to provide plasma residence times between approximately 250 μs and 1 ms. Measurements of temperatures, electron densities, and species concentrations were conducted by means of optical emission spectroscopy at locations 5 mm downstream of the exit plane of the nozzle (no test-section) and of the various test-sections. The measurements were performed using a SPEX model 750M, 3/4 meter, scanning monochromator fitted with a Hamamatsu model R1104 photomultiplier tube. Two 1200 lines/mm gratings blazed at 200 and 500 nm were used to cover the spectral range of the present study with an appropriate long pass filter to reject second order structures. Absolute intensity calibrations were obtained with two NIST traceable radiance standards: an Optronics model OL550 standard for wavelengths in 300-800 nm and a 1 kW Argon Mini-Arc from Arc Applications Research for the range 200-400 nm.

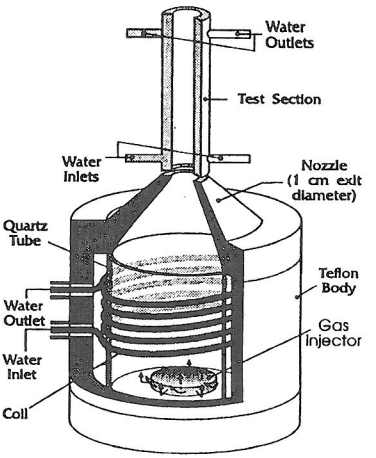

Figure 1. Schematic Cross-Section of Torch Head with Test-Section.

Results: Air Plasma

Temperature, electron density, and spectral emission measurements were performed at the exit of the nozzle (0 cm) and of the 15, 20 and 25 cm test-sections. Radial temperature profiles were obtained by Abel-inverting lateral profiles of the absolute intensity of the atomic oxygen triplet at 777.4 nm. Electron number densities were measured from the Stark broadening of the H_β line at 486.2 nm. To this end, a small quantity (1 slpm) of molecular hydrogen was premixed with 100 slpm of air before injection into the torch. Since electron concentrations are a maximum at the center of the plasma and drop rapidly with radial distance, the electron densities measured from line-of-sight H_β profiles should be very close to centerline values. The lineshapes were corrected for instrumental, Doppler and collisional broadening as was done in [5]. At each investigated location, the electron concentration was found to be within 10% of the equilibrium concentration at the measured temperature. Line-of-sight emission spectra were measured at 0, 15, and 20 cm and compared with equilibrium simulations performed with the radiation code NEQAIR2 [6,7] using the O-line temperature profiles. Differences between the measurements and the LTE simulations would be indicative of nonequilibrium conditions in the experiment. For instance, an overpopulation of N atoms would enhance radiation from the predissociating NO C state [5] and the Rayleigh-Lewis afterglow [8] from the N_2 B state. An overpopulation of N_2^+ would result in a corresponding increase of N_2^+ (B-X) radiation since, according to the collisional-radiative model of Park [9], the N_2^+ B state is in Boltzmann equilibrium with the ground state. However, at the three locations investigated, the equilibrium radiation calculations reproduced all measured spectral features originating from the B state of N_2^+, the B state of N_2, the A, B, and C states of NO, or the B state of O_2 within better than 25% (See Fig. 2 for the 20 cm case). The present measurements are therefore consistent with approximate LTE in the plasma.

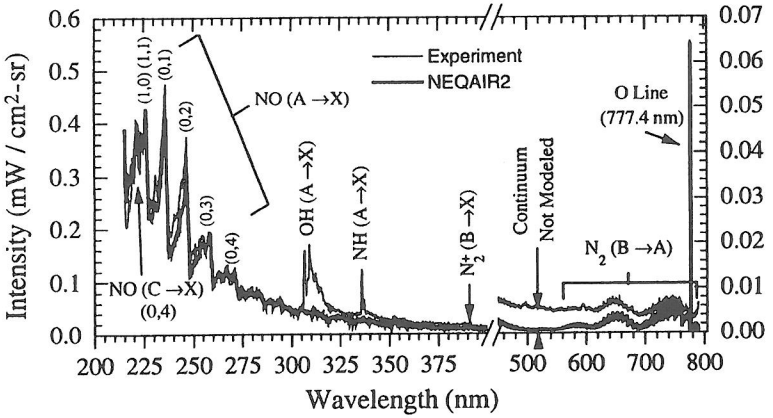

Figure 2. Measured and Computed Emission Spectra of the Air Plasma at 20 cm. The continuum-like structure between ~285 and 400 nm comprises diffuse bands from NO (B→X) and O_2 (B→X).

The kinetics code CHEMKIN [10] was used for one-dimensional modeling of the plasma chemistry along the axis of the flow. Diffusion effects were neglected. To calculate centerline velocities, the velocity and temperature profiles were assumed to be self-similar as the Prandtl number was calculated to be near unity. The velocity profiles were then scaled to match the 1.98 g/s mass flow rate of air/H_2. The centerline axial

velocity was found to decrease from 840 to 470 m/s between 0 and 25 cm. Species concentrations were computed using the axial temperature history thus determined. Nonequilibrium factors, noted ρ_s and defined as the ratios between the predicted and equilibrium concentrations of each species s, were computed with the reaction mechanisms of Dunn and Kang [2], Gupta et al.[3], and Park [4]. These factors are plotted versus reaction time in Fig. 3. A detailed analysis of these mechanisms reveals that: a) All charge exchange, charge transfer, and dissociative recombination reactions are fast and equilibrated. b) All three-body electron recombination reactions are slow. c) The main channel for electron recombination is the equilibrated dissociative recombination reaction of NO^+. It follows that $\rho_{NO+}\,\rho_e \cong \rho_N\,\rho_O$, and since NO^+ is the dominant ion and O atoms are close to equilibrium, $(\rho_e)^2 \cong \rho_N$. The electron overpopulation is therefore due to the N-atom overpopulation which itself arises because $N + O + M \Leftrightarrow NO + M$ and $2N + M \Leftrightarrow N_2 + M$ proceed at finite-rates. (Oxygen plays little role because it is almost entirely dissociated here; however, finite O-atom recombination rates control the chemistry at lower temperatures). This analysis holds qualitatively for the three reaction mechanisms. Quantitatively, the discrepancies between models are due to differences in the rates for $N + O + M \Leftrightarrow NO + M$ (with Park's rates being the largest). Since the present experimental results are consistent with the simulations based on Park's mechanism, this rate should be at least as fast as the rate proposed by Park in [4].

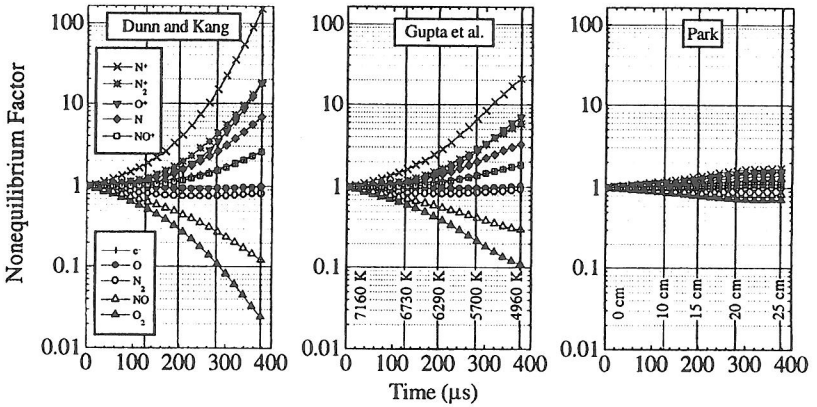

Figure 3. Nonequilibrium Factors Predicted by 3 Reaction Mechanisms for the Recombining Air Plasma.

Results: Nitrogen Plasma

High temperature nitrogen plasmas are notoriously more difficult to generate than air or argon plasmas because of their higher dissociation energy. For this reason, 50 slpm of argon was premixed to 100 slpm N_2 before injection into the torch. The rates for argon reactions being well known, measurement interpretations were not complicated by this additional gas. A small quantity (2.3 slpm) of H_2 was added for electron density determinations. Measurements were conducted at 0, 10 and 15 cm. Temperature profiles were measured from the Abel-inverted intensities of one argon (763.5 nm) and two hydrogen (H_α and H_β) lines, as well as from the Abel-inverted intensity of the band head of the N_2^+ (B-X) transition. At 0 and 10 cm, all temperatures agreed within 200 K, and the line-of-sight emission spectra recorded between 290 and 800 nm were reproduced within the 20% experimental uncertainty by equilibrium spectral simulations at the measured temperatures. In contrast, at 15 cm all temperatures were within 250 K of each other but the measured emission spectrum

could not be reproduced with any of the temperature profiles (see Fig. 4). Furthermore, while the measured electron overpopulation factors at 0 and 10 cm were found to be close to unity, at 15 cm an overpopulation factor of 15±5 was measured.

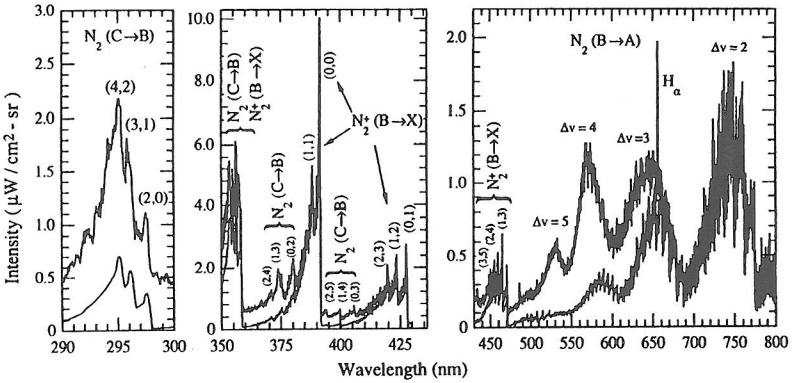

Figure 4. Measured (top curves) and Computed (bottom curves) Nitrogen Plasma Spectrum at 15 cm. (Note the good agreement for the B state of N_2^+ and the large differences for the B and C states of N_2.)

Numerical calculations were performed with CHEMKIN using the rates given by Park [4] for nitrogen chemistry and the rates of Table 1 for reactions with argon and hydrogen. The predicted nonequilibrium factors are shown on Fig. 5. Although N^+ is the main ion from 0 to 15 cm, electrons recombine primarily via the fast, equilibrated dissociative recombination reaction $N_2^+ + e \Leftrightarrow N + N$. The degree of ionizational nonequilibrium depends mainly on the rates of the (slow) reactions $2N + M \Leftrightarrow N + M$ (M = N, N_2). These rates are not very reliable as they were extrapolated from measurements above 8000 K for M = N and above 7000 K for M = N_2 [11].

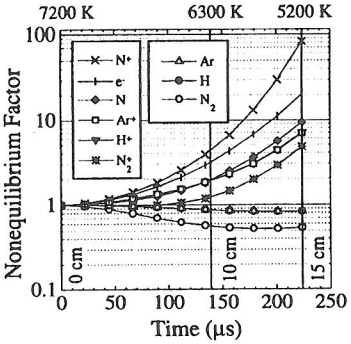

Fig. 5. Predicted Nonequilibrium Factors for Recombining Nitrogen/Argon Plasma.

The measured electron overpopulation factor at 15 cm is based on a temperature of ~5200 K determined from the N_2^+ band head intensity under the assumption of chemical equilibrium for N_2^+. If Park's model is correct, then N_2^+ is overpopulated by a factor ~5. Taking this factor into account, a new temperature can be determined from the N_2^+ band head profile. By repeating CHEMKIN simulations, a new value of the N_2^+ overpopulation factor is obtained. This iterative procedure converges to an N_2^+ overpopulation factor of 10 and a centerline temperature of 4820 K. To reproduce the experimental spectrum, the intensities of the vibrational bands of the N_2 C state must then be multiplied by a factor 32; for the B state of N_2, different factors must be used for different bands, with the largest for bands originating from v' = 10-12 (in accordance with the afterglow mechanism [8]). The electron overpopulation factor, now equal to 135±60, is consistent with but higher than the predicted value of 45. Clearly, N_2^+ concentration measurements are required to unambiguously determine the temperature and the various overpopulation factors. Also, measurements between 10 and 15 cm are needed. The accuracy of the nitrogen recombination rates will then be assessed.

Conclusions

In molecular plasmas, electron recombination occurs primarily through two-body dissociative recombination reactions. As a result, electron recombination rates are significantly greater than those for three-body electron recombination, and the extent of ionizational nonequilibrium is governed by the rates of relatively slow three-body atom recombination reactions such as $N + O + M \rightarrow NO + M$ and $2N + M \rightarrow N_2 + M$ in air and nitrogen plasmas. In order to test the predictions of three reaction mechanisms widely used for air plasma chemistry, measurements were made of electron and heavy particle concentrations in an air plasma forced to recombine from 7160 to 4900 K within 400 μs. These measurements indicated that LTE prevailed throughout the reaction zone, in good agreement with the predictions of one of the models [4] and thereby supporting a rate at least as fast as in [4] for $N + O + M = NO + M$. In experiments with a nitrogen plasma (with argon addition) forced to recombine from 7200 to 4700 K within 250 μs, significant chemical and ionizational nonequilibrium was observed. Predictions based on the model proposed in [4] were qualitatively consistent with these observations. Additional measurements are in progress to more quantitatively assess the extent of chemical nonequilibrium and the rate proposed in [4] for $2N + M \rightarrow N_2 + M$, and to determine how such effects as predissociation and electron excitation affect the population, hence the radiation, of excited N_2 states. This approach should lead to reliable rates for the reactions of importance in plasma recombination modeling and provide experimental data to test collisional-radiative models.

Table 1. Forward Rate Coefficients in Arrhenius Form: $A\,T^n \exp(-E/T)$

Reaction	A (cm^3/mol s)	n	E (K)	Ref	Remarks
$N_2 + Ar \Leftrightarrow N + N + Ar$	3×10^{21}	−1.6	113,200	11	
$Ar^+ + N_2 \Leftrightarrow Ar + N_2^+$	9×10^{11}	0.6	2,260	12	average of Ar^+ ($^2P_{1/2}$) and ($^2P_{3/2}$)
$H + e \Leftrightarrow H^+ + e + e$	1.51×10^{31}	−3.0	158,000	13	
$Ar^+ + e + e \Leftrightarrow Ar + e$	1.75×10^{21}	−1.0	−47,800	14	units of cm^6/mol^2 s
$H^+ + N \Leftrightarrow H + N^+$	2×10^{13}	0.5	0	15	taken same as $H^+ + O \Leftrightarrow H + O^+$

Acknowledgments

This research was supported by the Air Force Office of Scientific Research under the cognizance of Dr. Robert Barker, by means of grant AF-F49620-94.

References

1. Kruger, C.H., Owano, T.G., Gordon, M.H., Laux, C.O., *Pure Appl. Chem.* **64**, 607, 1992.
2. Dunn, M.G. and Kang, S.-W., *NASA CR-2232*, April 1973.
3. Gupta, R.N., Yos, J.M., Thompson, R.A., and Lee, K.-P., *NASA RP1232*, 1990.
4. Park, C., *J. Thermophys. Heat Transfer* **7**, 385, 1993.
5. Laux, C. O., Ph.D. Dissertation, *HTGL Report T-288*, Stanford University, 1993.
6. Laux, C.O., Moreau, S., and Kruger, C.H., *AIAA 92-2969*, 1992.
7. Laux, C.O., Gessman, R.J., and Kruger, C.H., *AIAA 93-2802*, 1993.
8. Partridge, H., Langhoff, S.R., Bauschlicher, C.W., *J. Chem. Phys.* **88**, 3174, 1988.
9. Park, C., *NASA TM 86707*, Ames Research Center, Moffett Field, CA 94035, 1985.
10. Kee, R.J., Rupley, F.M., Miller, J.A., *SAND89-8009*, Sandia National Lab., 1989.
11. Park, C., *AIAA 88-0458*, 1988.
12. Viggiano, A.A., Van Doren, J.M., Morris, R.A., Paulson, J.F., *JCP* **93**, 4761, 1990.
13. Kruger, C.H., *Plasma Chemistry and Plasma Processing* **9**, 435, 1989.
14. Owano, T.G., Kruger, C.H., and Beddini, R.A., *AIAA J.* **31**, 75, 1993.
15. Albritton, D.L., *Atomic Data and Nuclear Data Tables* **22**, 1, 1978.